Discover Oncology

Analysis

Single-cell RNA sequencing and traditional RNA sequencing reveals the role of cancer-associated fibroblasts in head and neck squamous cell carcinomas cohort

Ling Zhong[1] · Yixin Qiao[2] · Shasha He[1] · Yangju Fu[1] · Jian Zou[2]

Received: 19 February 2025 / Accepted: 25 April 2025
Published online: 23 May 2025

Abstract

Background Head and neck squamous cell carcinomas (HNSCs) are among the most common tumors worldwide. Despite the availability of various diagnostic and therapeutic strategies, the incidence and mortality rates of HNSC remain high. Cancer-associated fibroblasts (CAFs), as a major component of the tumor microenvironment, exhibit diverse biological characteristics in terms of origin, genetics, and phenotype, and have been increasingly recognized for their roles in tumor progression.

Methods To investigate the potential role of CAFs in HNSC, we performed a comprehensive bioinformatics analysis based on the TCGA HNSC cohort. We applied single-sample gene set enrichment analysis (ssGSEA), single-cell RNA sequencing (scRNA-seq) analysis, differential expression analysis, Cox regression, LASSO regression, and pathway enrichment analysis to identify CAF-related genes and assess their prognostic value.

Results We successfully identified a set of CAF-related genes and stratified the HNSC patients into high- and low-CAF groups. Based on the expression of these genes, we constructed a prognostic prediction model using LASSO and multivariate Cox regression analyses. A nomogram integrating the risk score and clinical characteristics was developed to improve individualized survival prediction. Enrichment analysis revealed that the type I interferon signaling pathway, cellular response to type I interferon, defense response to symbiont, and extracellular matrix organization were significantly associated with CAFs in HNSC.

Conclusion Our study provides a novel CAF-based prognostic model and nomogram for predicting patient outcomes in HNSC. These findings highlight the importance of CAFs in the tumor microenvironment and their potential as therapeutic and prognostic biomarkers.

Keywords Head and neck squamous cell carcinoma · Cancer-associated fibroblast · Immune cell infiltration · Single-cell RNA sequencing

1 Introduction

In 2018, the Global Cancer Report ranked head and neck squamous cell carcinomas (HNSCs) eighth in terms of commonness and death rate [1]. Local and distant failure after treatment for advanced HNSC occur in approximately 40% and 30% of patients, respectively, despite improvements in cancer patient survival over the last two decades

✉ Jian Zou, zoujian@wchscu.cn | [1]Department of Anesthesiology, West China Hospital, Sichuan University/West China School of Nursing, Sichuan University, Chengdu, Sichuan, China. [2]Department of Otolaryngology–Head & Neck Surgery, West China Hospital, Sichuan University, Chengdu, Sichuan, China.

[2]. There are multiple subsites of squamous cell cancer of the head and neck, including the oral cavity, oropharynx, hypopharynx, larynx, and nasopharynx [3]. Smoking and using tobacco-like products, as well as drinking alcohol, increase the risk of HNSC, which is well known [4]. As tobacco-derived carcinogens, excessive alcohol consumption, or both are associated with HNSC, the burden of the disease varies by country [5].

HNSCs have a tumor microenvironment (TME) that is composed of transformed cells, as well as components from the immune system and stroma [6]. Several studies of the TME have revealed critical roles for tumor-infiltrating immune cells in tumor dissemination, recurrence, metastasis, and immunotherapeutic response [7]. Among their tumor-promoting activities are immunosuppressive cytokines secreted by tumor-associated macrophages, which are associated with unfavorable outcomes [8]. Higher levels of tumor-infiltrating lymphocytes, such as CD4 + T cells and CD8 + T cells, were associated with improved survival and immunotherapy effectiveness conversely [9]. The treatment of head and neck squamous cell carcinoma with immune checkpoint inhibitors (ICI) has proven to be successful. There are, however, two major limitations of ICI therapy, namely the low rate of patient response and the high out-of-pocket costs [10]. Understanding the tumor microenvironment in HNSCC and identifying a biomarker to predict the efficacy of immunotherapy in patients with HNSCC are urgently needed [11].

The cancer-associated fibroblast (CAF) is an important part of the TME and exhibits a wide variety of biological characteristics, including cell origin, genetic makeup, and phenotype [12]. It is known that CAFs are derived from multiple types of cells and have increased expression of markers such as smooth muscle actin, fibroblast activation protein (PDGFR), and vimentin, which are all expressed in high levels [13]. Cancer-promoting effects are usually observed in most CAF subpopulations. Numerous previous studies have demonstrated that CAFs play an important role in multiple stages of tumor development [14]. Cancer cells achieve immune evasion through signaling mediated by CAF-derived cytokines within the TME, which not only promotes tumor proliferation but also induces cancer cell proliferation. There is still much to learn about the specific roles and mechanisms that CAFs play in cancer progression and pathogenesis [15].

A great deal of research has been conducted on cancer treatment over the past two decades, and the many breakthroughs have given us hope that many cancers will be successfully treated in the future. In the evolution of cancer immunotherapies and a better understanding of T cell responses to immune checkpoint inhibitors, we are developing precise biomarkers that can predict and identify precise genome-targeted drugs. The immune response to cancer is dynamic and variable, so identifying drugs that are useful in cancer immunotherapy requires more than just identifying a biomarker to identify patients who can benefit from immunotherapy. In order to determine whether the immune response affects clinical treatment, we need to evaluate the immune response. With the advancement of next-generation sequencing technologies, the biology of HNSC tumorigenesis and metastasis has become increasingly clear over the past few decades. In this work, we mainly focused the role of immunotherapy in HNSCCs patients. Several computational algorithms were used in this study to analyze the gene expression profiles of tumor samples and gain an understanding of the immune landscape. Also, the GO and KEGG enrichment pathways were also applied in the HNSC cohort to explore the potential pathways that are closely associated with immune-related characteristics.

2 Methods

2.1 Dataset downloaded

TISCH2 (Tumor Immune Single-cell Hub 2) is a scRNA-seq database dedicated to the tumor microenvironment. TME across different cancer types can be explored with TISCH2, which provides detailed cell type annotation at the single-cell level. In addition to meta-information, TISCH2 provides cell type annotation, expression visualization, differential gene expression, GSEA results, transcription regulator analyses, etc., for a single dataset. As of 2006, TCGA (The cancer genome atlas, Cancer Genome Atlas) is a joint project initiated by the National Cancer Institute and the National Human Genome Research Institute. A number of human cancers (tumors including subtypes) are represented in the TCGA database, which contains clinical data, genomic variations, mRNA expression, miRNA expression, methylation, among other data. In this work, the RNA-seq and the clinical-related information of HNSC patients was obtained from the TCGA database.

2.2 The differentially expressed analysis based on the R software

In the TCGA dataset (https://portal.gdc.com), the RNAseq data and associated clinical information of HNSC were obtained. We used R software's Limma package (version 4.0.2) to analyze mRNA expression differentially. To determine whether mRNA differential expression exists, P value < 0.05 and log2 (fold change) > 0.5 or log2 (fold change) < – 0.5 were used as the standard.

2.3 Single-sample Gene Set Enrichment Analysis (ssGSEA)

We used R v3.5.1, method = "ssgsea" to perform ssGSEA with the GSVA v1.30.0 package in GSVA v1.30.0. Our various immune cell signatures and other cell signatures were used to calculate NES. Each HNSC subtype was analyzed. For each HNSC subtype, expanded signatures that are unique to that subtype must be resolved to determine their enrichment significance. Our goal was to compare the NES for each subtype with the enrichment scores generated after 1000 permutations of randomly selected genes. For this analysis, all genes in the array were analyzed using a gene set of the same size as the extended signature. Furthermore, we performed a similar analysis with only the immune-related genes from ConsensusTME as input.

2.4 Gene ontology (GO) and Kyoto encyclopedia of genes and genomes (KEGG) enrichment analysis

In order to further confirm the potential functions of the potential targets, functional enrichment was used to analyze the data. The gene annotation tool GO is widely used for annotating genes with their functions, particularly molecular functions (MF), biological pathways (BP) and cellular components (CC). It is feasible to analyze gene function and related high-level genome function information using KEGG enrichment analysis. In order to better understand the oncogenic role of target genes, we analyzed GO functions of potential mRNAs and enriched KEGG pathways using the ClusterProfiler package in R.

2.5 The COX regression analysis was applied to construct the prognostic model

In the above analysis, the survival package of R software was used to construct the prognostic model using univariate and multivariate cox regression analyses. As part of the above analysis, the Least Absolute Shrinkage and Selection Operator (LASSO) regression algorithm was used, as well as tenfold cross-validation. The software used to do this analysis was the R package glmnet. In a data set in which log rank is used to test the KM survival curve distribution, the different groups are examined based on their KM survival curve distribution. The HR (High Risk) represents the risk coefficient of the high-risk group in comparison with the low-risk group. A model with HR greater than 1 is considered a risk model; a model with HR less than 1 is considered a protection model. It is the time when the high-risk group and low-risk group have equal survival rates, 95 percent CL. Median time is the time when the high-risk group and low-risk group have equal survival rates. An AUC value of more than 0.8 indicates a model that is more accurate at predicting survival times, in years. AUC curves and AUC values of a risk model at different times.

2.6 Immune cell infiltration analysis

In order to perform a reliable immune score evaluation, we used immunedeconv, an R package which incorporates several state-of-the-art immune-related algorithms, such as TIMER, xCell, MCP-counter, CIBERSORT, EPIC and quantIseq. In a systematic benchmarking process, each algorithm has been shown to possess its own unique properties and strengths. We then examine the expression of immune checkpoint-related genes and extract immune checkpoint-related gene expression values. In addition, TIDE algorithm was applied to evaluate the immune-related response of immunotherapy. The above mapping analysis uses the R software packages ggplot2 and ggpubr.

2.7 Genetic and clinicopathological features based on risk models

Based on the clinicopathological features of HNSC patients in TCGA database, we then performed the correlation analysis between risk model and clinicopathological features. In addition, the activation of immune-related pathways were also evaluate.

2.8 GSVA enrichment analysis

A comparison between KEGG pathways and Hallmark pathways was conducted using the R packages "GSVA" and "msigdbr" in order to understand differences in biological processes between subgroups. In order to study the relationship between immune cell infiltration among various subgroups, the ssGSEA algorithm was used. With the help of the R package "ggplot2", we visualized immune cell infiltration in different subgroups.

2.9 Cell culture

Human head and neck squamous cell carcinoma (HNSC) cell lines, SCC-9, were obtained from our lab. Cells were cultured in Dulbecco's Modified Eagle Medium (DMEM; Gibco, USA) or Minimum Essential Medium (MEM; depending on the cell line), supplemented with 10% fetal bovine serum (FBS; Gibco, USA), 1% penicillin–streptomycin (100 U/mL penicillin and 100 µg/mL streptomycin), and maintained at 37 °C in a humidified atmosphere containing 5% CO_2. The medium was replaced every 2–3 days, and cells were passaged using 0.25% trypsin–EDTA when reaching approximately 80–90% confluency.

2.10 shRNA construction and transfection

Short hairpin RNAs (shRNAs) targeting human were designed using online tools. The shRNA oligonucleotides were annealed and cloned into the pLKO.1-puro lentiviral vector according to the manufacturer's instructions. A non-targeting shRNA sequence was used as a negative control (sh-NC). For lentivirus production, HEK293T cells were co-transfected with the shRNA plasmid, psPAX2 (packaging plasmid), and pMD2.G (envelope plasmid) using Lipofectamine 3000 (Invitrogen, USA). Viral supernatants were collected 48 and 72 h post-transfection, filtered through a 0.45 µm filter, and used to infect target HNSC cells in the presence of 8 µg/mL polybrene. After 48 h, cells were selected with puromycin (2 µg/mL) for 5–7 days to establish stable knockdown cell lines. Knockdown efficiency was verified by quantitative real-time PCR and Western blotting.

2.11 RNA extraction and quantitative real-time PCR (qRT-PCR)

Total RNA was extracted from cultured cells using TRIzol™ Reagent according to the manufacturer's protocol. The concentration and purity of RNA were measured using a NanoDrop™ 2000 spectrophotometer. Reverse transcription was performed using a PrimeScript™ RT Reagent Kit with 1 µg of total RNA to synthesize complementary DNA (cDNA). Quantitative real-time PCR (qRT-PCR) was carried out using TB Green® Premix Ex Taq™ II on a QuantStudio™ 5 Real-Time PCR System. The relative expression levels of target genes were calculated using the $2^{-}\Delta\Delta Ct$ method, with GAPDH as the internal control. All reactions were performed in triplicate.

2.12 Cell proliferation assay (CCK-8 assay)

Cell proliferation was assessed using the Cell Counting Kit-8 following the manufacturer's instructions. Briefly, cells were seeded into 96-well plates at a density of 2×10^3 cells/well in 100 µL of complete medium. At the indicated time points, 10 µL of CCK-8 reagent was added to each well, and the plates were incubated for an additional 1–2 h at 37 °C.

The absorbance at 450 nm was measured using a microplate reader. All experiments were performed in triplicate, and the average absorbance values were used to plot cell growth curves.

2.13 Statistical analyses

It was considered statistically significant if the p-value < 0.05 was obtained when all statistical analyses were carried out with R software.

3 Results

3.1 The single-cell RNA sequencing analysis reveals the CAFs-related genes in HNSC patients

Firstly, we obtained the single-cell RNA sequencing dataset of GSE103322 from the TISCH2 database. In GSE103322, a total of 21 HNSC patients were involved. Subsequently, a total of 11 types of cells were involved in the GSE113322, which includes conventional CD4 T cells, CD8 T cells, CD8 exhaustion T cells, endothelial cells, fibroblasts, malignant cells, mast cells, mono cells, myocyte cells, myofibroblasts and plasma cells (Fig. 1A–D). The pie chart demonstrated the different proportion of the 11 type's cells in HNSC patients. Then, a total of 11 genes that are specially expressed in fibroblasts were considered as the CAFs in HNSC cohort, which involves ACTB, B2M, FTH1, HNRNPH1, SHISA9, MTRN2L1, MTRNR2L2, UGDH-AS1, MTRNR2L8, MTRNR2L10 and EEF1A1 (Fig. 1E–O).

3.2 The ssGSEA algorithm demonstrate the scores of immune-related indexes and fibroblasts

In order to explore the scores of immune-related indexes and fibroblasts in HNSC cohort, we then performed the ssGSEA algorithm. Subsequently, based on the immune-related indexes, the HNSC cohort was successfully divided into low- and high-immune-related groups (Fig. 2A, B). Multiple immune-related cells, immune-related functions and pathways were involved, which includes aDCs, AP -co-inhibition, APC co-stimulation, B cells, CCR, CD8 + T_cells, Check-point, Cytolytic activity, DCs, HLA, iDCs, Inflammation-promoting, Macrophages, Mast cells, MHC class I, Neutrophils, NK cells,

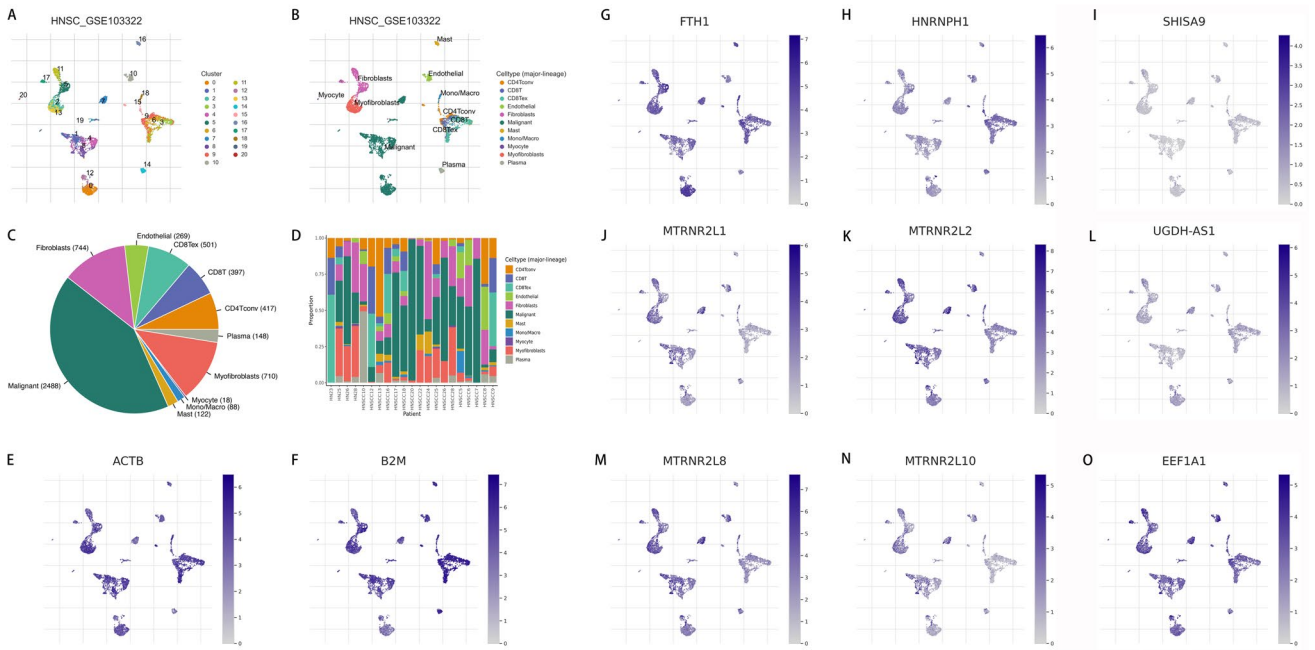

Fig. 1 **A** The results of cell clustering in single-cell RNA sequencing analysis. **B** The cell annotation of the single-cell RNA sequencing analysis. **C**, **D** The different distribution of the different cells in HNSC cohort; The expression level of ACTB (**E**), B2M (**F**), FTH1 (**G**), HNRNPH1 (**H**), SHISA9 (**I**), MTRNR2L1 (**J**), MTRNR2L2 (**K**), UGDH-AS1 (**L**), MTRNR2L8 (**M**), MTRNR2L10 (**N**) and EEF1A1 (**O**) in single-cell RNA sequencing

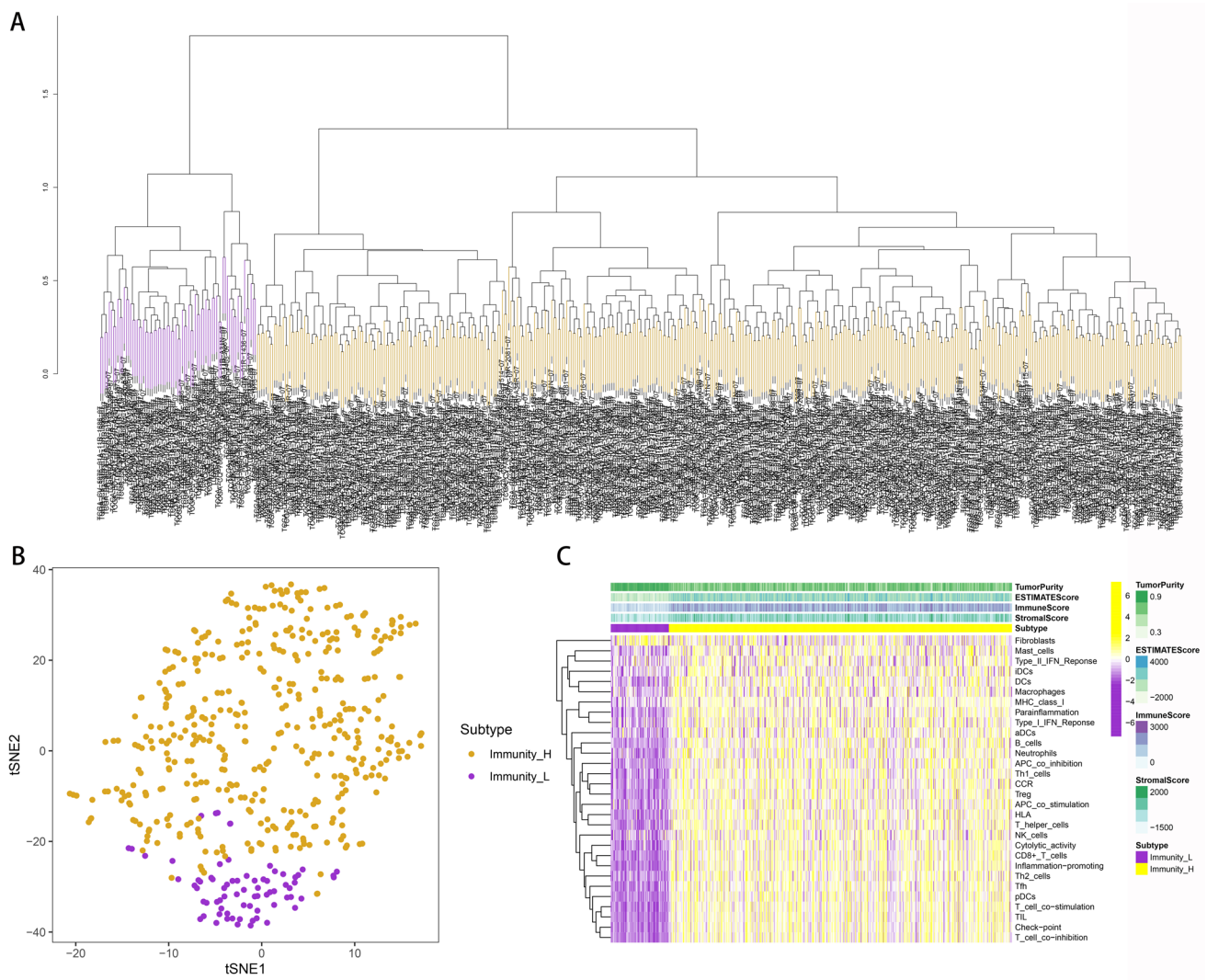

Fig. 2 **A** The analysis of ssGSEA algorithm based on the CAFs-related genes in HNSC cohort. **B** The different immune-related cohorts in HNSC cohort. **C** The heatmap demonstrated the expression of different immune-related cells, immune-related functions and fibroblasts

Parainflammation, pDCs, T cell co-inhibition, T cell co-stimulation, T helper cells, Tfh, Th1_cells, Th2_cells, TIL, Treg, Type I IFN Response, Type II IFN Response and Fibroblasts (Fig. 2C).

3.3 The immune-related subgroups were closely associated with the human leukocyte antigen (HLA)-related genes, TME and immune checkpoint-related genes

In addition, we also performed the correlation analysis between the immune-related subgroups and HLA-related genes, TME and immune checkpoint-related genes. In terms of TME, the results demonstrated that high-immune related groups are associated with the higher stromal score, immune score and estimate score (Fig. 3A). Also, we evaluate the role of HLA in HNSC cohort. Detecting antibodies in transplant candidates, detecting the level of this index to guide treatment, and improving prognosis can all be achieved using the HLA cell antigen (Fig. 3B). The correlation analysis revealed that HLA-related genes were closely associated with immune-related scores, which may indicate that immune-related score may guide treatment and improve prognostic indicators of HNSC patients. Finally, we also performed the correlation analysis between immune checkpoint-related genes and immune-related scores. In total, the higher immune-related scores are closely associated with the higher expression level of immune checkpoint-related genes (Fig. 3C). The term immune checkpoint refers to the programmed death receptors and their ligands. Through the blocking of programmed death receptors and their ligands, immune checkpoint blockade therapy increases tumor cell destruction by the immune

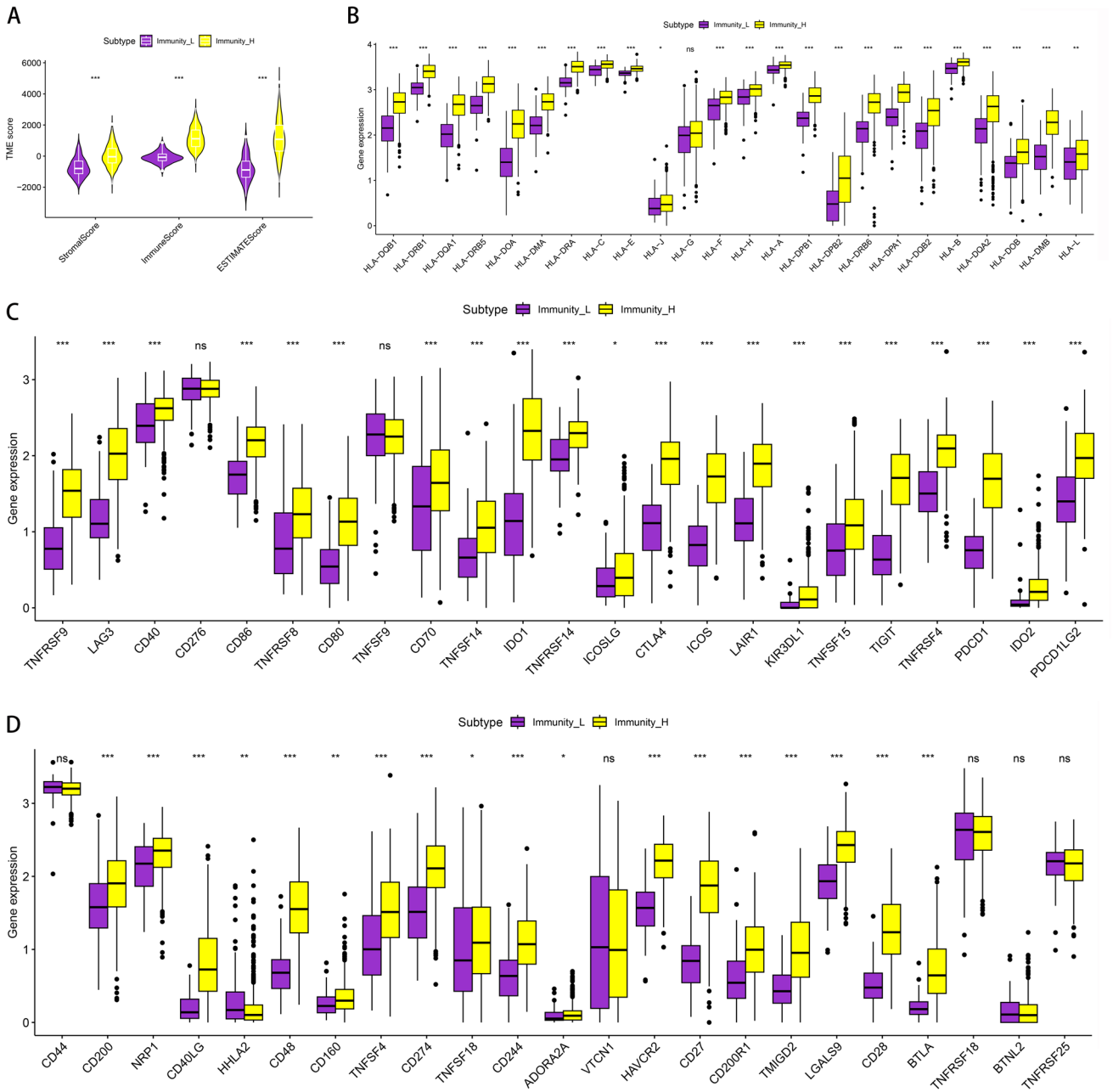

Fig. 3 **A** The correlation analysis between TMB and risk scores. **B** The correlation between HLA-related genes and risk scores. **C**, **D** The correlation analysis between immune checkpoint-related genes and risk scores

system. The results may suggest that the immune-related scores could guide the immune checkpoint-related therapy in HNAC cohort.

3.4 Evaluation of the CAFs-related genes and construction of the CAFs-related prognostic prediction model

On the basis of the ssGSEA algorithm, the HNSC cohort was successfully divided into low- and high-CAFs groups. We then performed the differentially expressed analysis. We finally obtained 112 up-regulated genes and 185 down-regulated genes, which were regarded as the key CAFs-related genes in HNSC cohort (Fig. 4A). In order to better explore the genes that are closely associated with the prognosis of HNSC patients, we then performed the cox regression analysis and lasso regression analysis. The univariate cox regression analyses demonstrated that a total of 21 genes may affect the prognosis of HNSC patients (Fig. 4B). We then performed the lasso regression analysis and multivariate cox regression

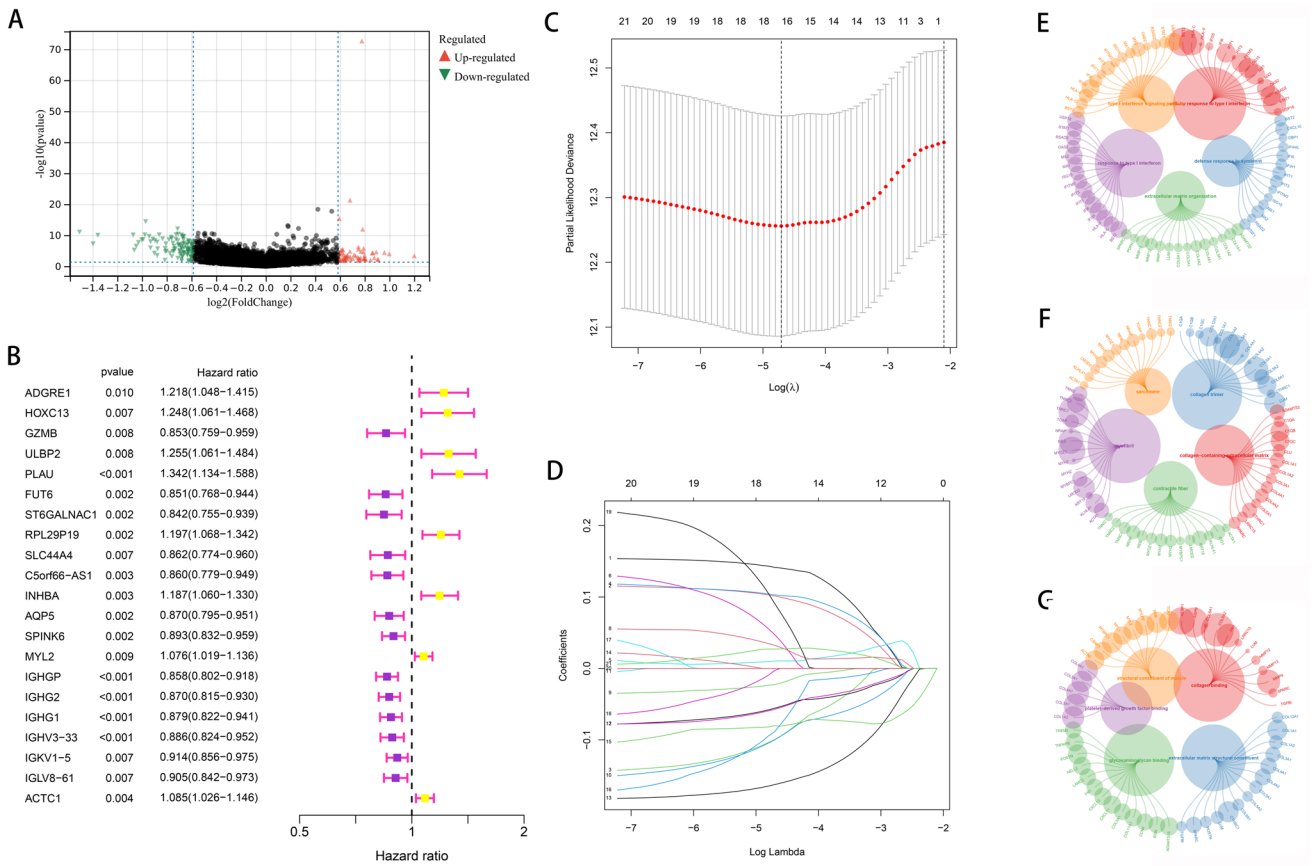

Fig. 4 **A** The different expressed analysis between low- and high-CAFs groups. **B** The univariate COX regression reveals the prognosis-related genes in different expressed genes. **C**, **D** The results of the lasso regression analysis. **E** The GO BP enrichment analysis. **F** The results of the GO CC enrichment analysis. **G** The results of GO MF enrichment analysis

analyses (Fig. 4C, D). At last, we successfully obtained a 8-genes based CAFs-related risk model. Also, we performed the GO enrichment analysis to explore the potential pathways that are closely associated with the 297 CAFs-related genes. For GO BP enrichment pathway, type I interferon signaling pathway, cellular response to type I interferon, response to type I interferon, defense response to symbiont and extracellular matrix organization were the most associated pathways (Fig. 4E). In addition, the GO CC enrichment pathways demonstrated that collagen-containing extracellular matrix, collagen trimer, contractile fiber, myofibril and sarcomere are the most associated pathways (Fig. 4F). Also, the GO MF enrichment pathways revealed that extracellular matrix structural constituent, collagen binding, platelet-derived growth factor binding, structural constituent of muscle and glycosaminoglycan binding are the most associated pathways (Fig. 4G).

3.5 Validation of the CAFs-related risk models in HNSC cohort

On the basis of the regression analysis, we successfully obtained the risk scores as follow: risk score = ADGRE1 * 0.166554950551384 + HOXC13 * 0.20695841235104 + GZMB * − 0.165857716575127 + C5orf66-AS1 * − 0.121679319581999 + AQP5 * − 0.0969209592105233 + SPINK6 * − 0.175120322153285 + IGHG2 * − 0.269214652593672 + IGKV1− 5 * 0.207295319560749. Each HNSC patients were assigned with a risk score. Based on the median risk score, the HNSC cohort was successfully divided into low- and high-risk groups (Fig. 5B). In addition, the survival analysis demonstrated that HNSC patients in high-risk group were associated with the poor overall survival (OS) (Fig. 5A). In order to compare the prognostic value between risk scores and clinical-related characteristics, we then performed the univariate and multivariate independent prognosis analysis. The results demonstrated that age, N stage and risk score are the risk factors in univariate independent prognosis analysis (Fig. 5C). Also, age, stage, T stage, N stage and risk score are the risk factors in multivariate independent prognosis analysis (Fig. 5D). Then, we used the ROC curve to evaluate the predictive value of risk model in HNSC cohort. The AUC score at 1-year, 3-year and 5-year are 0.667, 0.706 and

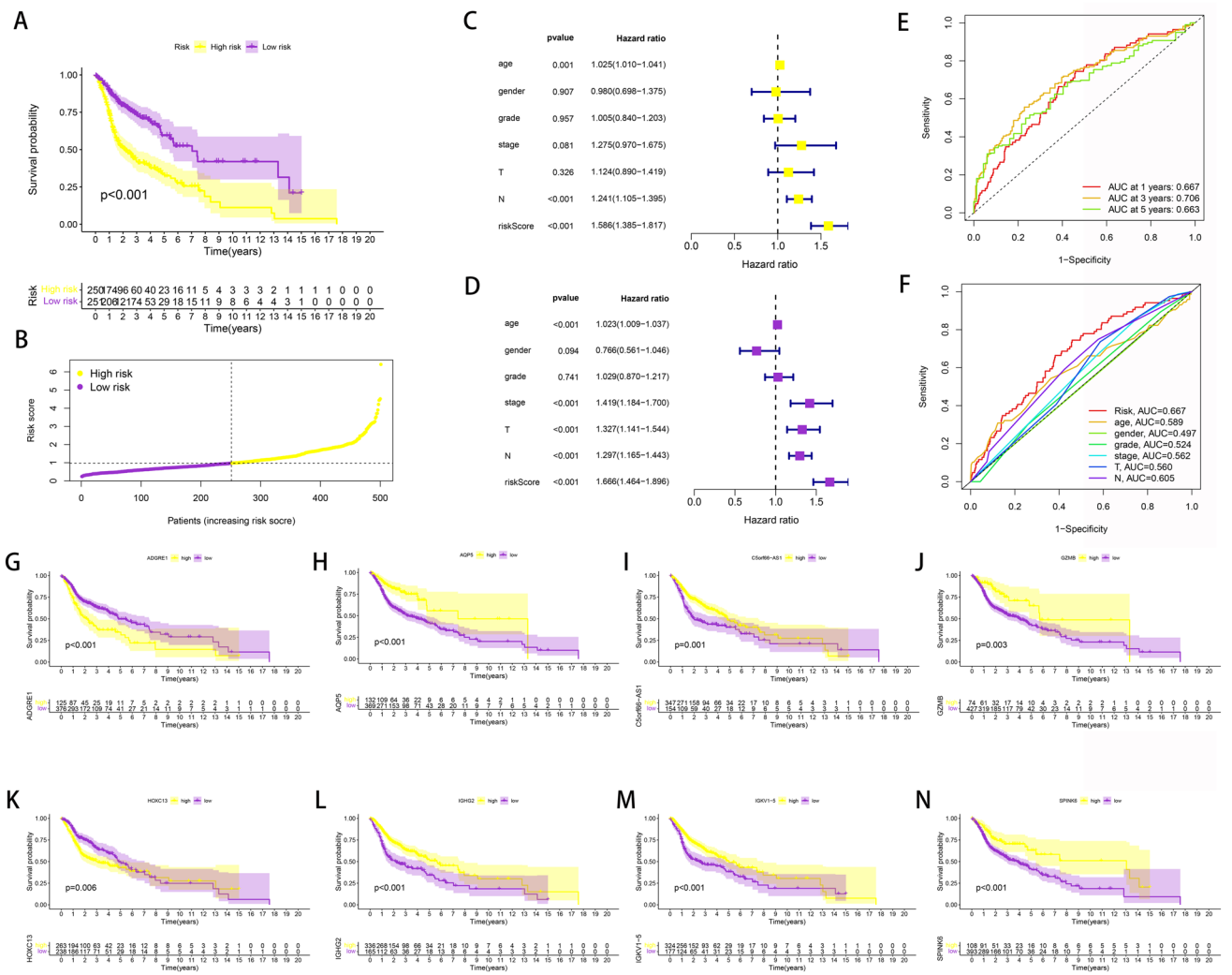

Fig. 5 **A** The survival analysis demonstrated the OS between low- and high-risk groups. **B** The risk plots based on the risk models. **C** The univariate independent prognosis analysis. **D** The multivariate independent prognosis analysis. **E** The time-dependent ROC curve. **F** The ROC curve based on the clinical-related characteristics and risk score; The survival analysis between the low- and high-expression level of AGDRE1 (**G**), AQP5 (**H**), C5orf66-AS1 (**I**), GZMB (**J**), HOXC13 (**K**), IGHG2 (**L**), IGKV1-5 (**M**) and SPINK6 (**N**)

0.663 respectively (Fig. 5E). In addition, ROC curve was also applied to compare the predictive value between risk model and clinical characteristics, such as age, gender, grade, stage, T stage and N stage. The AUC score for age, gender, grade, stage, T stage and N stage were 0.589, 0.497, 0.524, 0.562, 0.560 and 0.605 respectively (Fig. 5F). Finally, we performed the survival analysis based on the expression level of all 8 genes. The results demonstrated that the high expression level of ADGRE1 and HOXC13 were associated with the poor OS. However, the high expression level of GZMB, C5orf66-AS1, AQP5, SPINK6, IGHG2 and IGKV1-5 were associated with the good OS (Fig. 5G–N).

3.6 Construction of the nomogram based on the risk model and clinical-related characteristics

In order to obtain the predictive model with better predictive values, we then construct the nomogram by combining the risk score and clinical-related characteristics, which includes gender, grade, age, stage, T stage and N stage (Fig. 6A). The calibration curve proved that the nomogram shows good predictive value (Fig. 6B). Furthermore, we also performed the correlation analysis between clinical-related characteristics and risk score. The results demonstrated that HNSC patients with higher risk score are also correlated with higher age, higher grade, higher stage, higher T stage and higher N stage. Also, the male HNSC patients were also associated with the higher risk score (Fig. 6C–H).

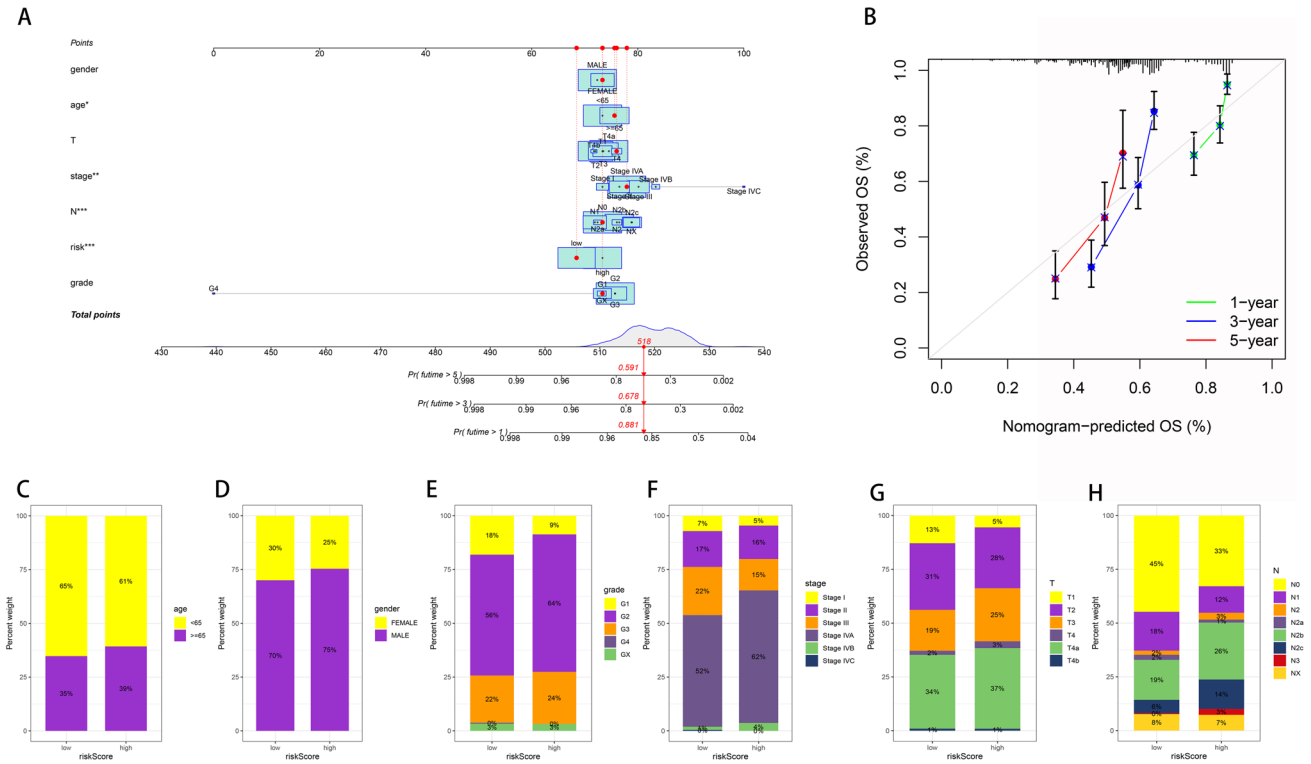

Fig. 6 **A** The nomogram based on the clinical-related characteristics and risk scores. **B** The calibration curve revealed the predictive value of nomogram; The correlation analysis between risk score and age (**C**), gender (**D**), grade (**E**), stage (**F**), T stage (**G**) and N stage (**H**)

3.7 The correlation analysis between risk model and immune-related cells, HLA-related genes and immune checkpoint-related genes

Based on the different immune-related algorithm, we then performed the immune cell infiltration analysis (Fig. 7A). The results demonstrated that CAF, M0 macrophage, M2 macrophage and NK are positively correlated with the risk score. In addition, B cell, CD8 + T cell, follicular helper T cell and M1 macrophage were negatively correlated with the risk score. Then, we also evaluate the association between risk score and HLA-related genes. Some HLA-related genes, which involves HLA-DQB1, HLA-DRB1, HLA-DRB5, HLA-DPB1, HLA-DPB2, HLA-DOB and HLA-DMB (Fig. 7B). In terms of the immune checkpoint-related genes, many are closely associated with the risk score, such as LAG3, CD276, CD86, TNFSF9, CD70, IDO1, TNFRSF14, CTLA4, ICOS, KIR3DL1, TIGIT, TNFRSF4, PDCD1, IDO2, PDCD1LG2, CD44, NRP1, CD40LG, CD48, TNFSF4, TNFSF18, CD244, CD27, TMIGD2, LGALS9, CD28, BTLA, TNFRSF18 and TNFRSF25 (Fig. 7C, D). The results suggests that HNSC patients with different risk scores may response differently to the immune checkpoint-related therapy.

3.8 ADGRE1 knockdown efficiency and its effect on cell proliferation

To investigate the role of ADGRE1 in HNSC cells, we first constructed stable knockdown cell lines using shRNA targeting ADGRE1. As shown in Fig. 8A, qRT-PCR analysis confirmed that the expression level of ADGRE1 was significantly reduced in the shADGRE1 group compared to the negative control group (shNC) ($P < 0.01$), indicating successful knockdown efficiency.

Next, we evaluated the impact of ADGRE1 knockdown on cell proliferation using the CCK-8 assay. As shown in Fig. 8B, there was no significant difference in cell viability between the shADGRE1 and shNC groups at day 0 and day 2. However, by day 4, cells transfected with shADGRE1 exhibited significantly higher OD450 values compared to the control group, suggesting that knockdown of ADGRE1 promoted cell proliferation in HNSC cells ($P < 0.01$).

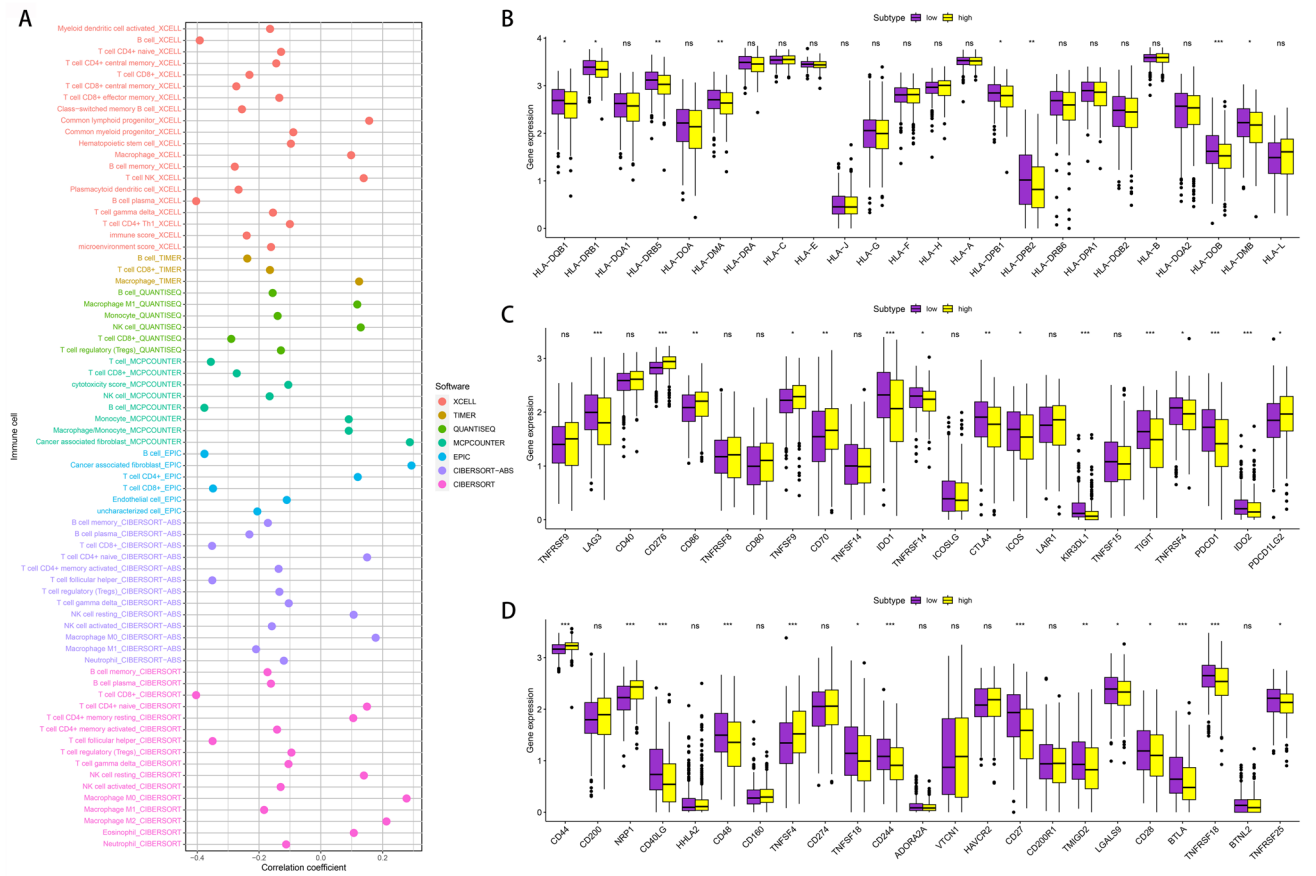

Fig. 7 **A** The immune cell infiltration analysis. **B** The correlation analysis between HLA-related genes and risk score **C**, **D** The correlation analysis between immune checkpoint-related genes and risk score

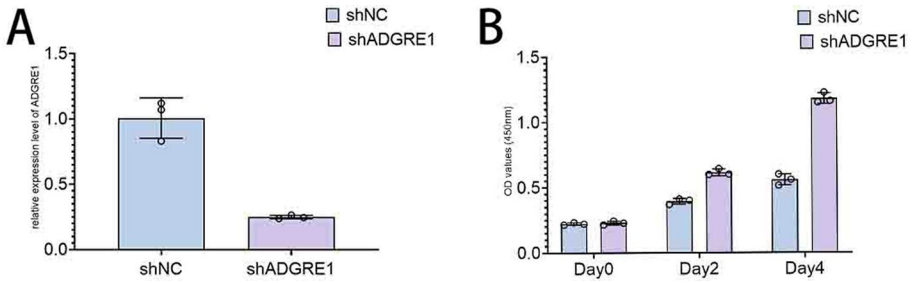

Fig. 8 Knockdown of ADGRE1 and its effect on cell proliferation in HNSC cells. **A** Quantitative real-time PCR (qRT-PCR) analysis of ADGRE1 mRNA expression levels in HNSC cells transfected with shRNA targeting ADGRE1 (shADGRE1) or negative control (shNC). ADGRE1 expression was significantly reduced in the shADGRE1 group compared to the shNC group. **B** Cell proliferation was measured using the CCK-8 assay at day 0, day 2, and day 4 post-transfection. Cells with ADGRE1 knockdown (shADGRE1) showed enhanced proliferation compared to control cells (shNC) at day 4. Data are presented as mean ± SD from three independent experiments. $P < 0.05$, $P < 0.01$

4 Discussion

HNSC is the sixth most common cancer in the world, accounting for 90% of all head and neck cancers, resulting in 650,000 cancer cases and 330,000 cancer deaths each year [16]. There have been many advances in surgery, radiation therapy, and systemic therapy, but the prognosis for HNSC patients remains poor [17]. In order to develop new therapies for HNSC, it is imperative to understand the cellular and molecular biology behind them. In addition to promoting tumorigenesis and increasing cancer cell invasiveness, CAF is an important component of TME stromal

cells [18]. A high degree of heterogeneity is observed in CAFs from a pathological standpoint. There have been several theories regarding the origins of this disease, including genetic changes in natural fibroblasts, tumor cell-mediated activation of pathological processes, and transdifferentiation of epithelial and mesenchymal cells [19]. As a result of excessive protein deposition and oncogenic molecules constantly secreted by CAFs, tumor cells invade, develop angiogenesis, become immunosuppressed, become resistant to drugs, and metastasize [20]. Consequently, targeting CAFs in conjunction with current tumor cell-targeting drugs may provide a synergistic therapeutic approach to counteract HNSC progression [21]. Therefore, in this work, we first performed the single-cell RNA sequence analysis to explore the fibroblast-related genes in HNSC cohort. Then, we performed the ssGSEA algorithm and differentially expressed analysis to obtain the CAFs-related genes. The different immune-related groups response differently to the HLA-related therapy and immune checkpoint-related therapy.

In order to further explore the prognostic value of CAFs-related genes, we then construct the prognostic prediction model in HNSC cohort based on the CAFs-related genes. A 8-genes signature based on the CAFs-related genes was used to predictive the prognosis of HNSC patients. Also, the independent prognostic analysis, ROC curve, nomogram, as well as the survival analysis demonstrated that the risk model shows good predictive value in HNSC cohort. In recent years, with the development of the bioinformatics analysis, more and more studies focused on the role of risk models in the prediction of treatment, diagnosis and prognosis. In recent years, advances in single-cell RNA-sequencing technology have generated a great deal of interest, enabling the profiling of genes and the identification of distinct oncogenic populations and associated markers [22]. The combination of single-cell RNA-sequencing technology and traditional RNA-sequencing technology provide a excellent tool to identify targets for more effective individualized management [23]. Our analysis revealed that the CAFs play a key role in the treatment, diagnosis and prognosis of HNSC patients. The ROC curve, nomogram and survival analysis all suggests that the risk model shows good predictive value in HNSC cohort.

Moreover, the pathways enrichment analysis provided us with the important pathways involved in the CAFs-related genes, such as type I interferon signaling pathway, cellular response to type I interferon, response to type I interferon, defense response to symbiont and extracellular matrix organization. Recent studies discovered that CD8 + T cells mediated by type I interferon promote antitumor immunity by activating MHC class I modified CD11b + dendritic cells [24]. Several studies have demonstrated that type I interferons (IFNs) inhibit tumor growth directly and indirectly by interacting with tumor cells and immune cells [25, 26]. As well, there is increasing evidence that the synergistic effects of endogenous and exogenous interferon enhancement on antitumor immunity are evident. It is important to note that type I interferons also play an important role in feedback inhibition of potential resistance to immunotherapy and antitumor immunity [27]. According to another study, the outcome of PD1 blockade therapy is determined by the precoded response of the peripheral immune system to type I interferon [28]. In total, our analysis may reveal that the CAFs may play a key role in the HNSC cohort via type I interferons-related pathways.

5 Limitations

Despite the comprehensive analysis conducted in this study, several limitations should be acknowledged. First, the data used in this study were primarily obtained from publicly available databases, such as TCGA and TISCH2, which may introduce selection bias. The heterogeneity of datasets, including differences in sequencing platforms, sample processing, and patient demographics, could influence the reproducibility and generalizability of our findings [29]. Second, our study relied on computational methods, including ssGSEA, Cox regression, and LASSO regression analyses, to identify CAF-related genes and construct prognostic models. While these approaches provide valuable insights, they require further experimental validation in independent patient cohorts and functional assays to confirm the biological relevance of the identified genes. Third, our study focused on the correlation between CAFs and immune-related features in HNSC but did not explore the dynamic interactions between CAFs and immune cells in the tumor microenvironment at a mechanistic level. Future studies using in vivo and in vitro experiments are necessary to elucidate the functional roles of CAFs in modulating tumor immunity and treatment responses. Lastly, the prognostic model developed in this study, while demonstrating good predictive value, should be further validated in prospective clinical trials to assess its utility in guiding personalized therapeutic strategies for HNSC patients.

Author contributions Ling Zhong write the manuscript. Yinxin Qiao and Shasha He analyzed the data. Yangju Fu and Jian Zou did experiment in the revised manuscript. All listed authors have made a significant scientific contribution to the research in the manuscript, approved its claims, and agreed to be an author. In addition, this is the finally version of authorship, the authorship will not be changed in the further process.

Funding This work was sponsored by corresponding author.

Data availability The datasets generated during and/or analyzed during the current study are available from the corresponding author on reasonable request.

Declarations

Competing interests The authors declare no competing interests.

References

1. Gu Z, Yao Y, Yang G, Zhu G, Tian Z, Wang R, Wu Q, Wang Y, Wu Y, Chen L, Wang C, Gao J, Kang X, Zhang J, Wang L, Duan S, Zhao Z, Zhang Z, Sun S. Pharmacogenomic landscape of head and neck squamous cell carcinoma informs precision oncology therapy. Sci Transl Med. 2022. https://doi.org/10.1126/scitranslmed.abo5987.
2. Moon DH, Sher DJ. Oligometastasis in head and neck squamous cell carcinoma. Int J Radiat Oncol Biol Phys. 2022;114(4):803–11. https://doi.org/10.1016/j.ijrobp.2022.06.086.
3. Harrington KJ, Burtness B, Greil R, Soulières D, Tahara M, de Castro G, Psyrri A, Brana I, Basté N, Neupane P, Bratland Å, Fuereder T, Hughes BGM, Mesia R, Ngamphaiboon N, Rordorf T, Wan Ishak WZ, Lin J, Gumuscu B, Swaby RF, Rischin D. Pembrolizumab with or without chemotherapy in recurrent or metastatic head and neck squamous cell carcinoma: updated results of the phase III KEYNOTE-048 study. J Clin Oncol. 2023;41(4):790–802. https://doi.org/10.1200/JCO.21.02508.
4. Li Z, Shen L, Li Y, Shen L, Li N. Identification of pyroptosis-related gene prognostic signature in head and neck squamous cell carcinoma. Cancer Med. 2022;11(24):5129–44. https://doi.org/10.1002/cam4.4825.
5. Chi H, Jiang P, Xu K, Zhao Y, Song B, Peng G, He B, Liu X, Xia Z, Tian G. A novel anoikis-related gene signature predicts prognosis in patients with head and neck squamous cell carcinoma and reveals immune infiltration. Front Genet. 2022;26(13):984273. https://doi.org/10.3389/fgene.2022.984273.
6. Burtness B, Rischin D, Greil R, Soulières D, Tahara M, de Castro G, Psyrri A, Brana I, Basté N, Neupane P, Bratland Å, Fuereder T, Hughes BGM, Mesia R, Ngamphaiboon N, Rordorf T, Wan Ishak WZ, Ge J, Swaby RF, Gumuscu B, Harrington K. Pembrolizumab alone or with chemotherapy for recurrent/metastatic head and neck squamous cell carcinoma in KEYNOTE-048: subgroup analysis by programmed death ligand-1 combined positive score. J Clin Oncol. 2022;40(21):2321–32. https://doi.org/10.1200/JCO.21.02198.
7. Chen J, Li K, Chen J, Wang X, Ling R, Cheng M, Chen Z, Chen F, He Q, Li S, Zhang C, Jiang Y, Chen Q, Wang A, Chen D. Aberrant translation regulated by METTL1/WDR4-mediated tRNA N7-methylguanosine modification drives head and neck squamous cell carcinoma progression. Cancer Commun. 2022;42(3):223–44. https://doi.org/10.1002/cac2.12273.
8. Jin S, Li M, Chang H, Wang R, Zhang Z, Zhang J, He Y, Ma H. The m6A demethylase ALKBH5 promotes tumor progression by inhibiting RIG-I expression and interferon alpha production through the IKKε/TBK1/IRF3 pathway in head and neck squamous cell carcinoma. Mol Cancer. 2022;21(1):97. https://doi.org/10.1186/s12943-022-01572-2.
9. Vos JL, Elbers JBW, Krijgsman O, Traets JJH, Qiao X, van der Leun AM, Lubeck Y, Seignette IM, Smit LA, Willems SM, van den Brekel MWM, Dirven R, Baris Karakullukcu M, Karssemakers L, Klop WMC, Lohuis PJFM, Schreuder WH, Smeele LE, van der Velden LA, Bing Tan I, Onderwater S, Jasperse B, Vogel WV, Al-Mamgani A, Keijser A, van der Noort V, Broeks A, Hooijberg E, Peeper DS, Schumacher TN, Blank CU, de Boer JP, Haanen JBAG, Zuur CL. Neoadjuvant immunotherapy with nivolumab and ipilimumab induces major pathological responses in patients with head and neck squamous cell carcinoma. Nat Commun. 2021;12(1):7348. https://doi.org/10.1038/s41467-021-26472-9.
10. Wise-Draper TM, Gulati S, Palackdharry S, Hinrichs BH, Worden FP, Old MO, Dunlap NE, Kaczmar JM, Patil Y, Riaz MK, Tang A, Mark J, Zender C, Gillenwater AM, Bell D, Kurtzweil N, Mathews M, Allen CL, Mierzwa ML, Casper K, Jandarov R, Medvedovic M, Lee JJ, Harun N, Takiar V, Gillison M. Phase II clinical trial of neoadjuvant and adjuvant pembrolizumab in resectable local-regionally advanced head and neck squamous cell carcinoma. Clin Cancer Res. 2022;28(7):1345–52. https://doi.org/10.1158/1078-0432.CCR-21-3351.
11. Yang L, Yu J, Tao L, Huang H, Gao Y, Yao J, Liu Z. Cuproptosis-related lncRNAs are biomarkers of prognosis and immune microenvironment in head and neck squamous cell carcinoma. Front Genet. 2022;22(13):947551. https://doi.org/10.3389/fgene.2022.947551.
12. Li X, Sun Z, Peng G, Xiao Y, Guo J, Wu B, Li X, Zhou W, Li J, Li Z, Bai C, Zhao L, Han Q, Zhao RC, Wang X. Single-cell RNA sequencing reveals a pro-invasive cancer-associated fibroblast subgroup associated with poor clinical outcomes in patients with gastric cancer. Theranostics. 2022;12(2):620–38. https://doi.org/10.7150/thno.60540.

13. Mao X, Xu J, Wang W, Liang C, Hua J, Liu J, Zhang B, Meng Q, Yu X, Shi S. Crosstalk between cancer-associated fibroblasts and immune cells in the tumor microenvironment: new findings and future perspectives. Mol Cancer. 2021;20(1):131. https://doi.org/10.1186/s12943-021-01428-1.
14. Chen Y, McAndrews KM, Kalluri R. Clinical and therapeutic relevance of cancer-associated fibroblasts. Nat Rev Clin Oncol. 2021;18(12):792–804. https://doi.org/10.1038/s41571-021-00546-5.
15. Li C, Teixeira AF, Zhu HJ, Ten Dijke P. Cancer associated-fibroblast-derived exosomes in cancer progression. Mol Cancer. 2021;20(1):154. https://doi.org/10.1186/s12943-021-01463-y.
16. Chen J, Lu T, Zhong F, Lv Q, Fang M, Tu Z, Ji Y, Li J, Gong X. A signature of N6-methyladenosine regulator-related genes predicts prognoses and immune responses for head and neck squamous cell carcinoma. Front Immunol. 2022;3(13):809872. https://doi.org/10.3389/fimmu.2022.809872.
17. Jin N, Keam B, Cho J, Lee MJ, Kim HR, Torosyan H, Jura N, Ng PK, Mills GB, Li H, Zeng Y, Barbash Z, Tarcic G, Kang H, Bauman JE, Kim MO, VanLandingham NK, Swaney DL, Krogan NJ, Johnson DE, Grandis JR. Therapeutic implications of activating noncanonical PIK3CA mutations in head and neck squamous cell carcinoma. J Clin Invest. 2021;131(22):e150335. https://doi.org/10.1172/JCI150335.
18. Luo H, Xia X, Huang LB, An H, Cao M, Kim GD, Chen HN, Zhang WH, Shu Y, Kong X, Ren Z, Li PH, Liu Y, Tang H, Sun R, Li C, Bai B, Jia W, Liu Y, Zhang W, Yang L, Peng Y, Dai L, Hu H, Jiang Y, Hu Y, Zhu J, Jiang H, Li Z, Caulin C, Park J, Xu H. Pan-cancer single-cell analysis reveals the heterogeneity and plasticity of cancer-associated fibroblasts in the tumor microenvironment. Nat Commun. 2022;13(1):6619. https://doi.org/10.1038/s41467-022-34395-2.
19. Foster DS, Januszyk M, Delitto D, Yost KE, Griffin M, Guo J, Guardino N, Delitto AE, Chinta M, Burcham AR, Nguyen AT, Bauer-Rowe KE, Titan AL, Salhotra A, Jones RE, da Silva O, Lindsay HG, Berry CE, Chen K, Henn D, Mascharak S, Talbott HE, Kim A, Nosrati F, Sivaraj D, Ransom RC, Matthews M, Khan A, Wagh D, Coller J, Gurtner GC, Wan DC, Wapnir IL, Chang HY, Norton JA, Longaker MT. Multiomic analysis reveals conservation of cancer-associated fibroblast phenotypes across species and tissue of origin. Cancer Cell. 2022;40(11):1392-1406.e7. https://doi.org/10.1016/j.ccell.2022.09.015.
20. Zhang C, Wang XY, Zhang P, He TC, Han JH, Zhang R, Lin J, Fan J, Lu L, Zhu WW, Jia HL, Zhang JB, Chen JH. Cancer-derived exosomal HSPC111 promotes colorectal cancer liver metastasis by reprogramming lipid metabolism in cancer-associated fibroblasts. Cell Death Dis. 2022;13(1):57. https://doi.org/10.1038/s41419-022-04506-4.
21. Kobayashi H, Gieniec KA, Lannagan TRM, Wang T, Asai N, Mizutani Y, Iida T, Ando R, Thomas EM, Sakai A, Suzuki N, Ichinose M, Wright JA, Vrbanac L, Ng JQ, Goyne J, Radford G, Lawrence MJ, Sammour T, Hayakawa Y, Klebe S, Shin AE, Asfaha S, Bettington ML, Rieder F, Arpaia N, Danino T, Butler LM, Burt AD, Leedham SJ, Rustgi AK, Mukherjee S, Takahashi M, Wang TC, Enomoto A, Woods SL, Worthley DL. The origin and contribution of cancer-associated fibroblasts in colorectal carcinogenesis. Gastroenterology. 2022;162(3):890–906. https://doi.org/10.1053/j.gastro.2021.11.037.
22. Hu D, Li Z, Zheng B, Lin X, Pan Y, Gong P, Zhuo W, Hu Y, Chen C, Chen L, Zhou J, Wang L. Cancer-associated fibroblasts in breast cancer: challenges and opportunities. Cancer Commun. 2022;42(5):401–34. https://doi.org/10.1002/cac2.12291.
23. Pan X, Zhou J, Xiao Q, Fujiwara K, Zhang M, Mo G, Gong W, Zheng L. Cancer-associated fibroblast heterogeneity is associated with organ-specific metastasis in pancreatic ductal adenocarcinoma. J Hematol Oncol. 2021;14(1):184. https://doi.org/10.1186/s13045-021-01203-1.
24. McNab F, Mayer-Barber K, Sher A, Wack A, O'Garra A. Type I interferons in infectious disease. Nat Rev Immunol. 2015;15(2):87–103. https://doi.org/10.1038/nri3787.
25. Crow MK, Olferiev M, Kirou KA. Type I interferons in autoimmune disease. Annu Rev Pathol. 2019;24(14):369–93. https://doi.org/10.1146/annurev-pathol-020117-043952.
26. Jiang J, Zhao M, Chang C, Wu H, Lu Q. Type I interferons in the pathogenesis and treatment of autoimmune diseases. Clin Rev Allergy Immunol. 2020;59(2):248–72. https://doi.org/10.1007/s12016-020-08798-2.
27. Sim TM, Ong SJ, Mak A, Tay SH. Type I interferons in systemic lupus erythematosus: a journey from bench to bedside. Int J Mol Sci. 2022;23(5):2505. https://doi.org/10.3390/ijms23052505.
28. Zitvogel L, Galluzzi L, Kepp O, Smyth MJ, Kroemer G. Type I interferons in anticancer immunity. Nat Rev Immunol. 2015;15(7):405–14. https://doi.org/10.1038/nri3845.
29. M Fan, B Geng, K Li, X Wang, and P K Varshney. Interpretable data fusion for distributed learning: a representative approach via gradient matching, in 2024. 27th International Conference on Information Fusion (FUSION). 2024: pp. 1–8.